Proceedings World Geothermal Congress 2015
Melbourne, Australia, 19-25 April 2015

Investigation of Injection-Triggered Slip on Basement Faults: Role of Fluid Leakoff on Post Shut-In Seismicity

Jack Norbeck and Roland Horne

Department of Energy Resources Engineering, Stanford University, Stanford, California, USA

jnorbeck@stanford.edu

Keywords: induced seismicity, triggered seismicity, basement faults, earthquake modeling

ABSTRACT

Several case studies of injection-triggered seismicity have suggested that the largest seismic events often occur in crystalline basement rock. In geothermal settings, the target reservoir is typically located in this type of rock. In wastewater disposal settings, crystalline basement rock is often considered a hydraulic barrier beneath the brine aquifer targeted for injection. Because earthquake magnitude is directly proportional to the surface area of the fault available for slip, it may not be surprising that the most significant earthquake activity is associated with the relatively large faults that can develop at greater depths in basement rock.

In this paper, we present a preliminary investigation of the physical mechanisms related to fluid injection in the subsurface that can affect slip on basement faults. We used a numerical model that coupled fluid flow in discrete faults and surrounding matrix rock, geomechanics, friction evolution, and permeability evolution to simulate earthquake behavior for a fault that had a direct hydraulic connection with an injection well. We were primarily interested in understanding the behavior following shut-in of the injection well. The numerical results indicated that it is very important to consider fluid leakoff from the fault zone into the surrounding matrix rock in order to more fully understand post shut-in seismic response. For the particular fault configuration modeled in this study, it was observed that significant post shut-in seismicity occurred for matrix permeabilities less than 10 μd. This type of post shut-in seismicity was attributed to pressure redistribution in the fault. Conversely, for matrix permeabilities greater than or equal to 10 μd, no significant post shut-in seismicity was observed. In the latter cases, fluid leakoff from the fault zone into the surrounding rock encouraged pressure dissipation within the fault, which overcame pressure redistribution effects within the fault zone. These results suggest that if significant post shut-in seismic activity is observed at a field site, then it is important to consider the contrast in permeability between the fault zone and matrix rock in order to determine whether pressure redistribution or some other mechanism (for example, thermoelasticity) is the dominant mechanism contributing to seismicity.

1. INTRODUCTION

Recently, several instances have been identified where fluid injection into the subsurface has been linked to relatively large earthquakes that were felt at the earth's surface in both the geothermal and oil and gas sectors (McGarr, 2015). Seismic events associated with injection of subsurface fluids have been documented in the scientific literature for several decades. Seismicity occurs when the frictional resistance to slip is overcome by the shear tractions acting on a fault, causing patches of the fault to fail in shear. If the frictional properties of the fault generally exhibit velocity-weakening behavior, then shear slip perturbations can cause a cascading loss of frictional strength across the fault resulting in unstable earthquake rupture events. The majority of case studies and theoretical investigations of injection-triggered seismicity have focused on the role of increased pore pressure in fault zones as a mechanism for reducing the effective normal stress acting on faults and thereby reducing their frictional resistance to slip. This mechanism requires a direct hydraulic connection between an injection well and a fault in order for the pressure within the fault zone to be perturbed significantly.

We performed numerical experiments that simulated fluid injection directly into a permeable fault located in low-permeability basement rock. The purpose was to investigate how fluid leakoff from the fault zone affects earthquake activity during injection and following shut-in of the injection well. If pressurization of the fault zone is indeed the dominant mechanism causing seismicity at a given site, then the seismic behavior will be influenced by the contrast in permeability of the fault zone and the surrounding matrix rock. Our goal was to determine whether a critical value of matrix permeability existed that discouraged post shut-in seismicity.

Additional mechanisms may contribute significantly to fault slip in certain circumstances. Changes in the solid stresses in the earth can arise due to poroelastic effects, thermoelastic effects, or mechanical deformation of faults. In contrast to the reduction in simple effective stress due to increased pore pressure, these changes in solid stress are transferred through the reservoir elastically, and therefore may contribute to seismic activity in regions that were not directly subjected to pore pressure or temperature perturbations. Based upon the results of the numerical experiment, we speculate whether other mechanisms might be important to consider in future analyses.

This paper is organized as follows. In Section 2, we present a brief review of several case histories of injection-triggered seismicity in order to illustrate the motivation for this work. In Section 3, we show the results from a numerical experiment of injection into a planar fault that has relatively high permeability with respect to the surrounding matrix rock. The primary goal of the experiment was to determine how fluid leakoff from the fault affects the seismic activity following shut-in of the well. In Section 4, we provide a discussion of the numerical results and propose directions for future research in this area.

2. REVIEW OF SEVERAL CASE HISTORIES OF INJECTION-TRIGGERED SEISMICITY

The purpose of this paper is purely to elucidate several physical mechanisms that are important to consider when designing or monitoring water injection projects. Earthquakes are typically regarded as natural phenomena, so it is extremely difficult to discern

whether anthropogenic activity has caused seismicity in many cases. Nonetheless, it is a useful exercise to review several case histories where significant seismicity has occurred in close proximity to injection wells in order to identify commonalities or differences between the geologic settings and operational conditions at the sites. Here, we review four case histories of sites where it has been suggested that injection may have triggered seismic activity.

2.1 Rocky Mountain Arsenal, Denver, Colorado, USA

One of the earliest reports of injection-triggered seismicity was at the Rocky Mountain Arsenal wastewater disposal project in the 1960's (van Poollen and Hoover, 1970). Injection into a 3.6 km deep well located near Denver, Colorado, USA began in 1962. At the time this well was completed, it was unique because it was targeting faulted and fractured crystalline basement rock as the injection zone. It was also the deepest wastewater disposal well at the time. Roughly 625,000 m^3 of fluid were injected over the five-year period from 1962 to 1966. The first seismic event was recorded in 1962, and over 100 earthquakes large enough to be felt at the surface occurred in the following years. The well was ordered to be shut-in in 1966, and at that point the United States Geologic Survey installed a seismic array at the site. In 1967, following shut-in of the well, the three largest earthquakes were recorded (magnitudes 4.8, 5.1, and 5.3). In their report, van Poollen and Hoover (1970) suggested that thermal stresses generated by injection of relatively cool water were likely to be more significant than pore pressure perturbations at most spatial scales throughout the reservoir and over the majority of the duration of injection.

2.2 Guy, Arkansas, USA

More recently, the central and eastern United States have observed a marked increase in the number of seismic events greater than M 3.0 (Ellsworth, 2011). It has been proposed that some of these events may be related to the disposal of wastewater. One such case occurred in the area near Guy, Arkansas, USA. Eight injection wells used to dispose of hydraulic fracturing wastewater became active starting in April 2009. The area has experienced seismic activity in the past, with recent seismic swarms in nearby Enola, Arkansas in 1981 and 2001. After the start of injection in 2009, the rate of seismic events with magnitudes greater than 2.5 rose significantly. Horton (2012) reports that there was "one in 2007, two in 2008, 10 in 2009, 54 in 2010, and 157 in 2011," and that 98% of the earthquakes originated less than 6 km from the injection wells. Several large steeply dipping normal faults near the injection sites were well known and did not become active during the injection. Rather, the recent seismicity was observed to form a very strong linear trend, suggesting the activation of a previously unidentified fault in the basement rock beneath the target injection aquifer. This shallowly dipping strike-slip fault is roughly 15 km long and is well oriented for shear in the current stress state in the region. Horton (2012) suggested that the largest earthquake that could occur along this fault is M 5.7, based on the estimated surface area of the fault. In February 2011, a M 4.7 earthquake occurred along the newly identified Guy-Greenbriar fault (Horton, 2012; Zoback, 2012). Subsequently, the two wells closest to the fault were shut-in. The earthquakes did not stop, but the rate and size of the earthquakes did drop. A third well was shut-in voluntarily by the operator, and a fourth well was ordered to be shut-in by the Arkansas Oil and Gas Commission. At least six small earthquakes have been recorded following shut-in of these injection wells (Horton, 2012).

2.3 Basel, Switzerland

In engineered geothermal systems (EGS), the reservoir is typically stimulated in order to increase permeability. The most widely applied EGS reservoir stimulation technique has been to target fault zones during drilling, and then inject fluid in an attempt to cause shear slip on preexisting fractures and faults. This process, called shear stimulation, intends to permanently increase reservoir permeability through breakdown of mineral seals and natural propping of fracture and fault planes. In 2006, a geothermal well was drilled in the city of Basel, Switzerland for the purpose of developing a geothermal cogeneration plant. The well was drilled to a depth of roughly 5 km into granitic basement rock. In order to enhance the permeability of the reservoir, the well was stimulated by injecting a total of 11,500 m^3 of water over a period of six days (Mukuhira et al., 2008). Although the stimulation was scheduled to last for 21 days, microseismic activity during the initial six days was severe enough to cause authorities to suspend injection based upon a pre-defined seismic response procedure (Häring et al., 2008). Prior to shut-in, the largest event was M 2.8. About five hours after shut-in, the largest event of M 3.4 was recorded. Following this event, the well was bled-off. Three events of magnitude greater than 3.0 were recorded over the next two months (Majer et al., 2007; Häring et al., 2008). The project was ultimately cancelled in 2009.

2.4 St. Gallen, Switzerland

In the summer of 2013, a geothermal well near St. Gallen, Switzerland was subjected to a stimulation treatment program. The stimulation targeted a zone at a depth of 4.0-4.5 km. Preliminary injection tests indicated a low level of risk for a significant seismic event (Kraft et al., 2014). Shear stimulation proceeded, but the required level of stimulation was not achieved through the initial efforts. Subsequently, an acidization procedure was implemented. During the acid job, the well sustained a natural gas kick, and heavy mud was immediately injected in order to kill the well. During this time, the intensity and magnitudes of events increased. On July 20, 2013, a M 3.6 event occurred that was located to a depth of 4 km (Swiss Seismologic Service, 2013). Over 400 residents within a 15 km radius of the site reportedly felt the event. The seismicity rate decreased following production tests that were performed after the M 3.6 event. Although this geothermal well was not completed in granitic basement rock, this case study is particularly interesting because a traffic light system was in place to prevent exposure to seismic risk, but the requirement to kill the well during the gas kick precluded the ability of the operator to shut-in the well even though seismic activity was increasing.

2.5 Discussion

The four case studies discussed above provide several interesting insights. The first observation is that the largest events tended to occur in granitic basement rock. At Guy, Arkansas, the largest event occurred in the basement rock below the target aquifer. Because the seismic moment release during an event is proportional to the surface area available for slip, it is not surprising that large basement faults may be responsible for creating the most significant events. In many cases it is difficult or impossible to use seismic imaging techniques to identify faults in basement rock, so it may be prudent to develop alternative strategies to identify the existence of potentially threatening basement faults. Another observation is that the largest event often occurred following shut-in of the well. This is a somewhat unintuitive observation given that pore pressures are generally expected to decrease in a diffusion-

driven process in an infinite domain. This suggests that the relatively simple conceptual model of increased pore pressure in an effective continuum may not always be applicable, even as a first-order approximation, to the problem of slip on a fault. Finally, given the complex geologic settings and the unique operating conditions at each of these field sites, it is arguable that, in addition to the simple effective stress concept, alternative physical mechanisms such as poroelastic and thermoelastic effects may be playing significant roles in the observed seismicity.

3. INJECTION INTO A FAULT: DIRECT HYDRAULIC CONNECTION

Injection-triggered seismicity is typically modeled as a Mohr-Coulomb failure process, in which slip occurs if the shear tractions acting on a fault exceed the frictional resistance to slip. Fault slip can be considered negligible under the following condition:

$$\tau + \Phi - \eta V \leq f\left(\sigma_n - p\right) + S, \tag{1}$$

where τ is the shear stress acting on the fault, Φ is the elastic stress transfer that develops due to gradients in shear slip along the fault, η is a radiation damping parameter used to approximate inertial effects, V is the sliding velocity of the fault, f is the coefficient of friction for the fault, σ_n is the normal component of the solid stress in the earth resolved on the fault plane, p is the pore pressure in the fault zone, and S is the cohesion of the fault surface. Compressive stress is taken as positive in this sign convention.

If a direct hydraulic connection exists between an injection well and a fault, then the pore pressure within the fault zone can be altered. One practical example of this conceptual model is the Basel geothermal well, in which the well penetrated a fault zone that had a relatively high permeability with respect to the surrounding rock. Another possible scenario for this type of behavior is if injection is occurring into a faulted domain in which the fault permeability is on the same order as that of the intact rock. An example of this type of behavior may be the Guy, Arkansas wastewater disposal site, in which one possible explanation for the large seismic events is that a basement fault penetrated the target injection aquifer in close proximity to the injectors. In contrast, if fault permeability is much lower than the intact rock, then this mechanism is not expected to be significant because pore pressure will not easily diffuse into the fault rock.

At the Basel geothermal site and the Rocky Mountain Arsenal wastewater disposal site, the largest seismic events occurred following shut-in of the injection wells. Baisch et al. (2010) and McClure and Horne (2011) provided insightful explanations for this phenomenon. These authors argued that during injection, pore pressures in the fault zone are highest near the well and a negative pressure gradient exists away from the well. Upon shut-in, the pressure quickly equilibrates such that pore pressures near the edges of the fault continue to increase for a short duration. If the reservoir rock surrounding the fault zone is sufficiently impermeable to prevent significant fluid leakoff and the volume of injected fluid is large enough with respect to the fault's storativity, then the effect of the pressure redistribution can be to cause patches near the edge of the fault to slip. In the numerical experiment that follows, we are interested primarily in the post shut-in seismic behavior.

3.1 Numerical Model Scenario

We performed a numerical modeling study to investigate the role of the surrounding matrix rock permeability in encouraging fluid pressure dissipation within the fault zone after shut-in. For this study, we used a reservoir simulator that coupled fluid flow in discrete faults and surrounding matrix rock, fracture mechanics, and friction evolution (McClure, 2012; Norbeck et al., 2014; Norbeck and Horne, 2014). Fluid exchange between the discrete faults and intact matrix rock was performed using an embedded fracture modeling strategy (Li and Lee, 2008; Norbeck et al., 2014). Friction evolution was modeled using a rate and state friction framework (Segall, 2010). For details on the coupling between fluid flow, geomechanics, and friction evolution the reader is referred to McClure and Horne (2013) and Norbeck and Horne (2015).

We considered a vertical strike-slip fault oriented 20° clockwise from the direction of maximum principal stress. The injection well was assumed to penetrate the fault directly in the center of the fault, and flow was assumed to be essentially one-dimensional in the long direction of the fault. The fault was 50 m high, 500 m long, and 10 cm wide. The fault porosity was 7%. The initial permeability distribution along the fault was slightly heterogeneous and was maintained the same for each simulation. The fault permeability was on the order of several hundred darcies. An illustration of the fault geometry is shown in Fig. 1. All relevant model parameters for the fault, including rate and state friction parameters, are given in Table 1. The model parameters for the reservoir rock are given in Table 2. Initial pore pressure was constant in space throughout the reservoir at 40 MPa. The maximum and minimum principal stress magnitudes were 100 and 65 MPa, respectively. Various matrix permeabilities were tested in order to identify the effects of fluid fleakoff in the seismic response following shut-in. The well injected water at a constant mass flow rate of 10 kg/s unless a maximum injection pressure of 59 MPa was reached, whereupon constant injection pressure was maintained at that level (see Table 3). In this manner, injection pressures were maintained well below the minimum principal stress for the entire duration of all simulations. The simulations were isothermal.

Three cases were simulated in order to model fluid leakoff effects in low matrix permeability settings. The matrix permeabilities for each case were 0 μd, 1 μd, and 10 μd, respectively. In order to encourage significant pressure redistribution following shut-in, injection was continued until a relatively large percentage of the fault had experienced stimulation. In each simulation, injection was halted after seven discrete earthquake events occurred, corresponding to roughly 80% of the fault experiencing slip. Seismic activity was monitored following shut-in until the pressure distribution within the fault was constant (for the case with zero leakoff) or returned to initial conditions (for the two cases with leakoff).

Earthquake moment magnitudes were calculated as:

$$M_0 = G \int_A \delta \, \mathrm{d}A, \tag{2}$$

where M_0 is the earthquake moment magnitude, G is shear modulus, δ is the cumulative shear slip discontinuity during an event, $\mathrm{d}A$ is the surface area of an elemental section of the fault, and A is the total surface area of the fault patch that slipped. In our model, the fault was essentially a two-dimensional plane, and slip occurred only in one direction. Moment magnitudes were likely overestimated compared to real earthquakes, because slip was assumed to be constant along each vertical cross-section. Note that the permeability distribution along the fault was slightly heterogeneous in order to overcome the common observation that earthquake events tend to propagate along the entire fault using rate and state models with homogeneous faults. The simulation results were therefore not expected to be perfectly symmetric.

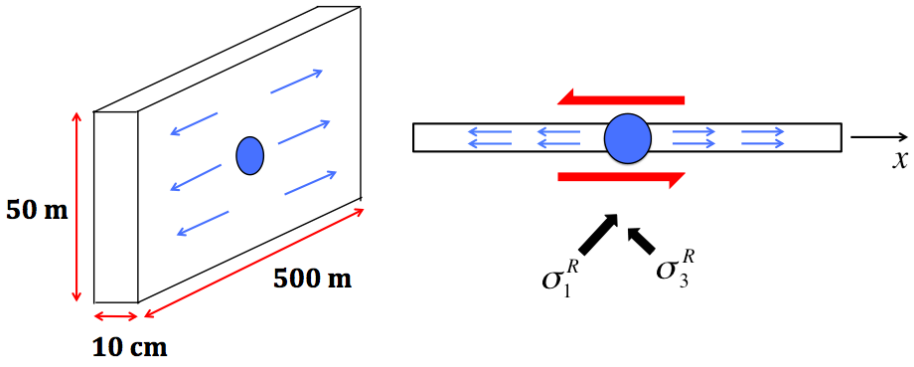

Figure 1. Schematic of the model fault. The injection well intersected the fault at the center of the fault.

Table 1. Model parameters related to the vertical fault.

Fault Model Parameters

Parameter	Value	Unit
L^f	500	m
H^f	50	m
W^f	10	cm
ϕ^f	0.07	-
k^f	> 100	d
f_0	0.6	-
a	0.011	-
b	0.014	-
v_0	1×10^{-9}	$\mathrm{m \cdot s^{-1}}$
θ_0	1×10^{7}	s

Table 2. Model parameters related to the matrix rock.

Reservoir Model Parameters

Parameter	Value	Unit
k^m	0 to 10	μd
ϕ^m	0.08	-
p_0	40	MPa
σ_1	100	MPa
σ_3	65	MPa
G	15	GPa
ν	0.2	-

Table 3. Model parameters related to the well controls.

Well Control Model Parameters

Parameter	Value	Unit
m^{wf}_{max}	10	$\mathrm{kg \cdot s^{-1}}$
p^{w}_{max}	59	MPa

3.2 Numerical Model Results

Three simulations were performed using different values of matrix permeability. In Case 1 the matrix permeability was zero, in Case 2 the matrix permeability was 1 μd, and in Case 3, the matrix permeability was 10 μd. Summaries of the number of earthquakes observed and their corresponding magnitudes for each case are given in Table 4. For each case, a total of seven seismic events were observed prior to shut-in. The magnitudes of each event were comparable between cases during injection. Following cessation of injection, Case 1 had three earthquakes, Case 2 had two earthquakes, and Case 3 had zero earthquakes. For this fault configuration, it was concluded that the critical matrix permeability that allowed pore pressure in the fault zone to diffuse quick enough to prevent post shut-in events was roughly 10 μd. This is a very low permeability for traditional oil and gas resources, but may be representative for crystalline basement rock.

Table 4. Summaries of the simulated earthquake events observed for a) Case 1, b) Case 2, and c) Case 3.

$k^m = 0$		$k^m = 1\,\mu d$		$k^m = 10\,\mu d$	
EQ #	**Magnitude**	**EQ #**	**Magnitude**	**EQ #**	**Magnitude**
1	1.74	1	1.73	1	1.70
2	0.87	2	0.98	2	1.04
3	1.51	3	1.55	3	1.60
4	1.66	4	1.69	4	1.75
5	1.79	5	1.82	5	1.88
6	1.91	6	1.94	6	2.00
7	2.00	7	2.05	7	2.09
8	1.19	8	1.47	N/A	
9	0.39	9	1.23		
10	0.72				

During Injection
Post Shut-In

(a) **(b)** **(c)**

The simulations provided the necessary insight to diagnose three distinct types of earthquake behavior related to the mechanism of interest for this paper: pressurization of fluid in the fault zone through a direct hydraulic connection between the fault and the well. The evolution of various fault parameters for three representative earthquake events are shown in Figs. 2 - 4. The fault parameters of interest are pore pressure in the fault zone, cumulative shear displacement along the fault, sliding velocity along the fault, and shear stress acting on the fault. Because we modeled a perfectly planar fault, shear slip did not cause any perturbation in normal stress acting on the fault. Additionally, we neglected the poroelastic effect due to fluid leakoff. Therefore, the normal component of the solid stress acting on the fault remained constant throughout the duration of all simulations, and the effective stress is purely a function of pore pressure within the fault zone. The plots represent any horizontal cross-section along the vertical dimension of the fault, i.e., the x-direction goes with the long direction of the fault. The temporal evolution of each property is illustrated using shaded lines. The darkest line represents the beginning of the event, and the lines become lighter with increasing time. The best way to visualize the nucleation and cessation of the earthquake event is to observe the temporal evolution of sliding velocity.

A typical earthquake event during the injection period is illustrated in Fig. 2. This event corresponds to earthquake #7 from Case 1. During constant rate injection, pore pressures are continually increasing along the fault. One of the most striking characteristics of this type of event is that shear slip was able to propagate across the entire previously stimulated region. The events tended to nucleate near the edges of the previously stimulated region, and then propagate towards the center. Simultaneously, the edge of the stimulated region extended towards the edge of the fault. The earthquake ruptures arrested because the rupture fronts were propagating into areas of increasing effective stress. Relatively low shear stress values in the stimulated region are indicative of the stress drop released during the earthquakes. Slip velocity tended to reach its highest value at the moment when slip was transferred across the entire fault. Cumulative shear slip tended to increase rapidly when this occurred. From Tables 4a and 4b, it is clear that event magnitudes associated with this type of event were relatively large compared to the events that occurred post shut-in. This indicates that for large events to occur, slip must be able to propagate across a significant portion of the fault.

A representative temporal sequence for a post-shut in seismic event is shown in Fig. 3. This event corresponds to earthquake #8 from Case 1, but the two post shut-in events for Case 2 showed qualitatively similar earthquake rupture behavior. Following shut-in of the injection well, pressure in the fault tends to redistribute if the matrix permeability is sufficiently low to prevent fluid leakoff from the fault. Pressure near the well decreases and pressure near the edges of the fault actually increases as the pressure attempts to equilibrate. This effect was described previously by Baisch et al. (2010) and McClure and Horne (2011) as a mechanism for triggering post shut-in earthquakes. Compared to the types of events that occurred during injection, the main difference for this type of event was that slip was unable to propagate across the entire fault. As was observed in the other type of event, the earthquakes tended to nucleate near the edges of the fault. However, the relatively low pore pressure near the center of the fault contributed to a relatively large frictional resistance to slip (see Eq. 1), which caused the event to die out. As indicated in Tables 4a and 4b, the post shut-in events tended to be smaller in magnitude than the events that occurred prior to shut-in.

In Fig. 4, we show an example of an event sequence following shut-in for Case 3, the case with the highest matrix permeability. In this case, the relatively large amount of fluid leakoff from the fault was enough the allow pore pressure in the fault zone to dissipate quick enough to prevent any post shut-in events from occurring. Compared with the previous type of event (i.e., post shut-in earthquakes), it is clear that the pressure gradients are shallower, and that relatively low pressure exists over a broader distance along the fault. During this event, the sliding velocity history indicates that an event was attempting to nucleate due to pressure redistribution effects, but eventually died out before reaching a state of unstable slip. Incremental shear displacement was relatively small and was confined to the edges of the stimulated region. In this type of event, the competition between pressure redistribution within the fault and the ability of the surrounding matrix rock to accept fluid leakoff evidently favored leakoff effects.

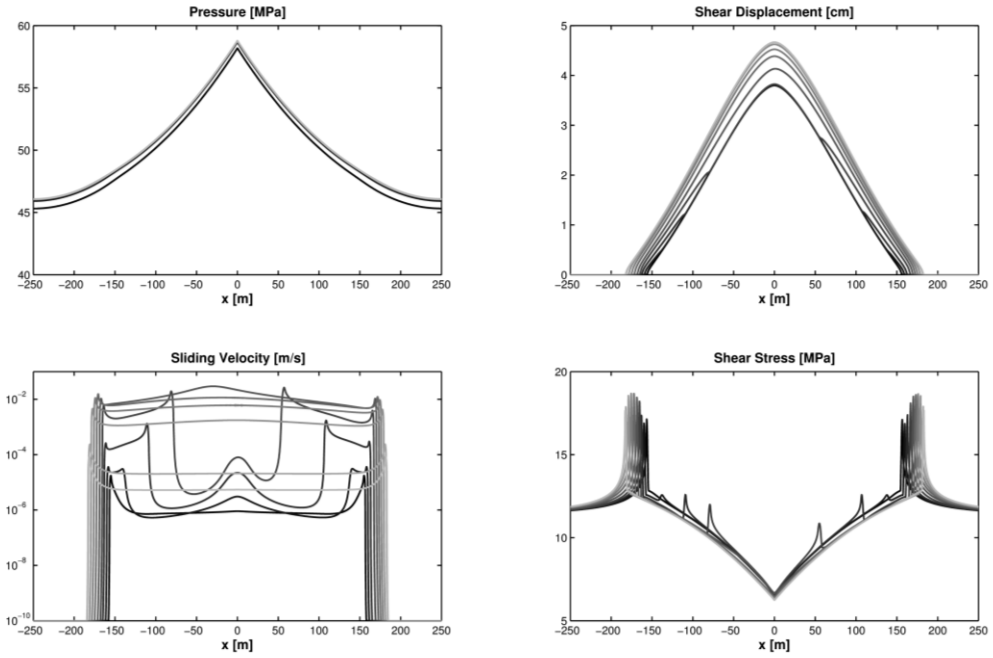

Figure 2. A representative temporal sequence of an earthquake event during injection (i.e., prior to shut-in). The darkest black line marks the start of the event, and the lines become progressively lighter over the duration of the event. The main characteristic is that slip was transferred across the entire previously stimulated region of the fault during the event.

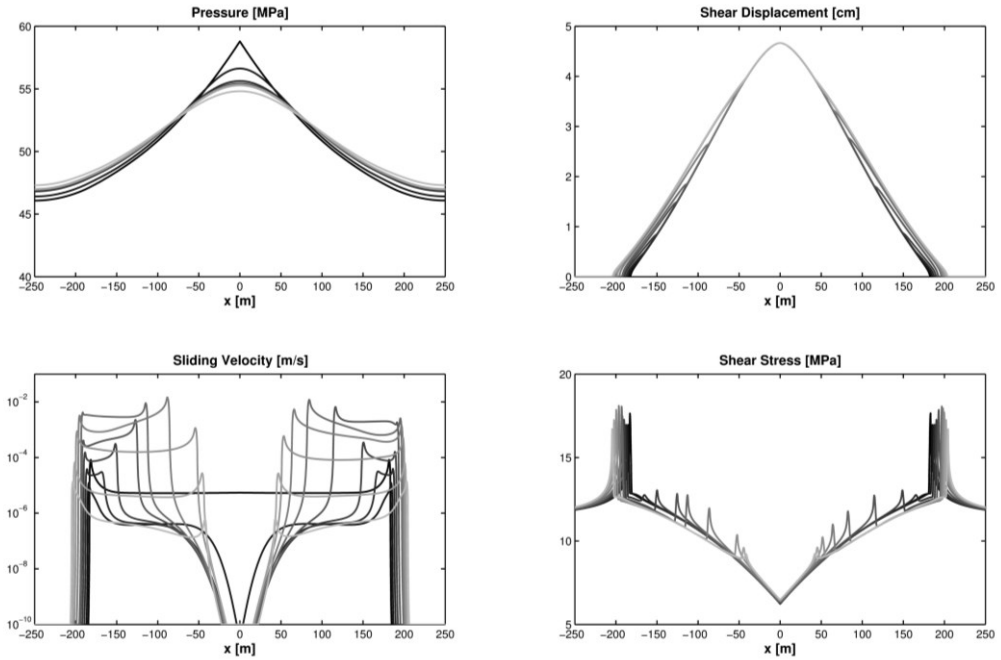

Figure 3. A representative temporal sequence for a post shut-in earthquake event for settings with relatively low matrix permeability. The darkest black line marks the start of the event, and the lines become progressively lighter over the duration of the event. During this type of event, slip was localized toward the edges of the fault. Slip did not propagate across the entire previously stimulated region because the combination of relatively low pore pressure and relatively large stress drop near the center of the fault inhibited shear failure.

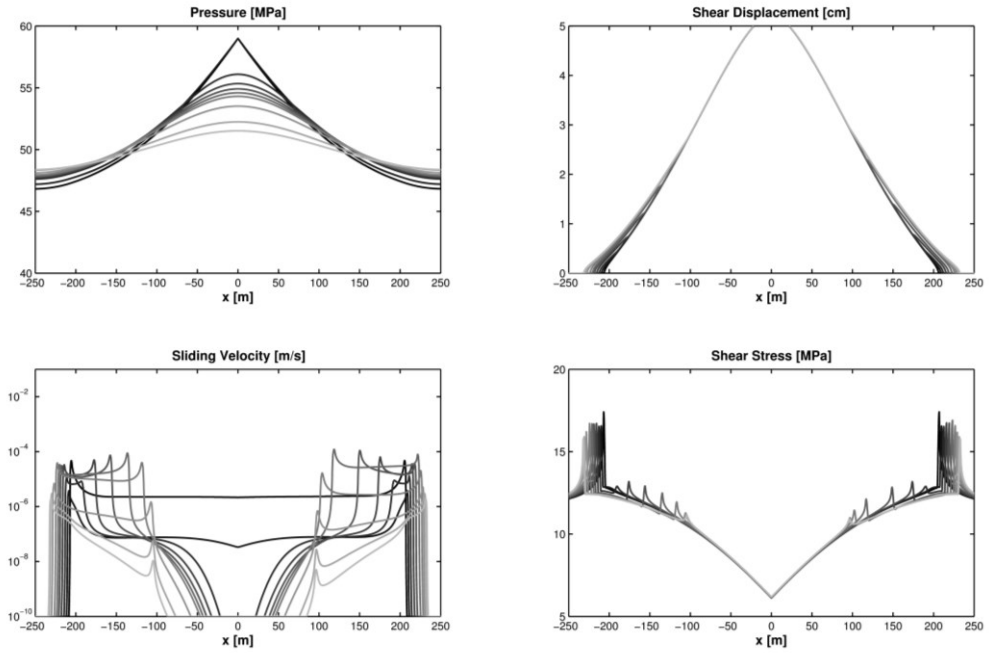

Figure 4. A representative temporal sequence of earthquake behavior post shut-in for settings with relatively high matrix permeability. The darkest black line marks the start of the event, and the lines become progressively lighter over the duration of the event. In this case, pore pressure redistribution in the fault is competing with the surrounding matrix rock's ability to store fluid. The pore pressure is not able to redistribute fast enough, and the potential earthquake is unable to nucleate due to high fluid leakoff.

4. DISCUSSION AND CONCLUDING REMARKS

In this paper, we focused on one particular physical mechanism that can contribute to injection-triggered seismicity. We used numerical modeling to investigate the scenario where a fault has a direct hydraulic connection with an injection well. This conceptual model is reflective of several case studies (Basel, Switzerland and Guy, Arkansas, USA) where injection may have caused triggered seismic events in granitic basement rock. In this scenario, pore pressure within the fault zone is increased during injection, which can lead to a reduction in effective stress and, consequently, a reduction in the frictional resistance to slip. This is the most common mechanism attributed to causing injection-triggered seismicity.

We were primarily interested in the slightly more complex behavior following shut-in of the injection well. Several case studies indicated that significant seismicity occurred after the well was shut-in, and in some cases the largest earthquakes occurred post shut-in. Baisch et al. (2010) and McClure and Horne (2011) suggested that pressure redistribution could cause post shut-in events upon. McClure and Horne (2011) presented numerical results that confirmed this hypothesis by modeling a fault surrounded by matrix rock that was impermeable.

In this work, we investigated how the permeability of the matrix rock affected the ability for pressure within the fault zone to redistribute. We modeled direct injection into a vertical fault surrounded by matrix rock with various values of permeability. Higher values of matrix permeability encouraged fluid leakoff from the fault zone into the surrounding rock, thereby allowing pressure within the fault to dissipate more quickly. For the fault configuration that we modeled, we found that a critical matrix permeability of 10 μd prevented post shut-in seismicity. This numerical experiment demonstrated that, depending on the geologic environment, pore pressure redistribution within the fault zone might not always be responsible for post shut-in seismicity.

A thorough review of the geologic settings at the field sites discussed in Section 2 was not performed for the purposes of this paper. However, if matrix permeability was high enough to discourage pore pressure redistribution within the fault zones at these sites, then that would suggest that the observed post shut-in seismicity was caused by other mechanisms. Under the assumption of relatively high fluid leakoff from the fault zone, thermoelasticity and poroelasticity are two physical processes that should be considered.

Neglecting poroelastic effects in the surrounding rock for the moment, the change in effective normal stress due to pressurization within the fault zone and an instantaneous cooling of the fault zone due to injection of relatively cold fluid is (Jaeger et al., 2007):

$$\Delta\sigma_n^{'} = -\alpha\Delta p + \frac{3(1-2\nu)}{1-\nu}\beta K\Delta T, \tag{3}$$

where $\Delta\sigma_n^{'}$ is the change in effective normal stress, α is Biot's coefficient, Δp is the change in pore pressure within the fault zone, ν is Poisson's ratio, β is linear thermal expansion coefficient of the rock, K is bulk modulus, and ΔT is the change in temperature of the fault zone. Typical values for the rock properties are on the order of $\alpha \approx 1$, $\nu \approx 0.25$, $\beta \approx 10^{-5}$ °C^{-1}, and $K \approx 10$ GPa. For injection of fluids at ambient conditions into a reservoir with a natural geothermal gradient at 4 km depth, the

temperature change might be $\Delta T \approx -50$ °C. Looking at the second term on the right hand side of Eq. 3 related to thermal effects, the change in normal stress given the parameters listed above would be $\Delta\sigma_n' = -10$ MPa. If the fault and reservoir permeability were high enough such that pore pressure perturbations were not significant, then it is clear that thermal effects could be the dominant factor causing seismicity. As the cooling front propagates away from the fault, more of the reservoir volume undergoes thermal contraction. This effect would tend to further decrease the effective normal stress acting on the fault. Upon shut-in of the injection well, the pore pressure will equilibrate relatively quickly. On the other hand, the cooling front is able to continue propagating away from the fault due to thermal conduction even after shut-in. This suggests that thermal effects may have contributed significantly to seismic activity in cases where seismicity was observed to occur well beyond shut-in.

The poroelastic effect due to increased fluid pressure in the surrounding matrix rock during injection would tend to cause an increase in the solid normal stress acting on the fault. This effect would discourage slip. Upon shut-in, fluid pressures in the surrounding rock would tend to dissipate back towards initial reservoir pressure, relieving the temporary increase in solid normal stress. Of course, pore pressure within the fault zone would also be dissipating (or at least equilibrating) after shut-in. Norbeck and Horne (2015) performed numerical simulations that included additional poroelastic and thermoelastic stresses. In general, they reported that poroelastic stresses due to fluid leakoff tended to have a stabilizing effect and thermoelastic stresses due to reservoir cooling tended to have a destabilizing effect.

The discussion so far has been limited to the case where a fault is located within a region of perturbed pore pressure or temperature. It is also useful to consider the non-local stress perturbations that arise due to the fact that stresses are transferred elastically through the reservoir. A useful conceptual model to help gain an understanding of this type of phenomenon is called the Eshelby inclusion model (Eshelby, 1957). In this model, an elliptical region of rock is subjected to a set of strains (e.g., due to cooling or pore pressure changes) and the stress perturbations in the surrounding rock are calculated. The resulting stress distributions can be quite complex, unintuitive, and geometry dependent. The stress perturbations fall off relatively quickly with distance away from the inclusion. However, under the theory of a critically stressed crust, very small changes in effective stress ($\Delta\sigma_n' < 1$ MPa) have been reported to trigger earthquakes.

From this discussion, it is apparent that several physical mechanisms are able contribute to injection-triggered seismicity. The interaction and competition between these processes must be more fully understood in order to manage situations in which triggered seismicity occurs or is expected to occur. In general, the significance of each mechanism is extremely case dependent and is subject to geologic setting and operating conditions. Future research in this area will involve the development of a numerical model that couples the following physical processes: fluid flow in faults and surrounding matrix rock, heat transfer, poroelasticity, thermoelasticity, friction evolution, and permeability evolution. This work warrants further parametric study to determine the ranges of geologic and operational parameters over which various triggering mechanisms dominate.

REFERENCES

Baisch, S., Vörös, R., Rothert, H., Stang, H., Jung, R., and Schellschmidt, R. 2010. A numerical model for fluid injection induced seismicity at Soultz-sous-Forêts. *International Journal of Rock Mechanics and Mining Sciences,* **47** (3): 148-158. doi: 10.1785/01200080055.

Ellsworth, W.L. 2011. Injection-induced earthquakes. *Science*, **341** (6142). doi: 10.1126/science.1225942.

Eschelby, J.D. 1957. The determination of the elastic field of an ellipsoidal inclusion, and related problems. *Proc. R. Soc. Lond. A.* **241**: 376-396. Doi: 10.1098/rspa.1957.0133.

Häring, M.O., Schanz, U., Ladner, F., and Dyer, B.C. 2008. Characterisation of the Basel 1 Enhanced Geothermal System. *Geothermics,* **37** (5): 469-495. doi: 10.1016/j.geothermics.2008.06.002.

Horton, S. Disposal of hydrofracking waste fluid by injection into subsurface aquifers triggers earthquake swarm in central Arkansas with potential for damaging earthquake. *Seismological Research Letters,* **83** (2): 250-260. doi: 10.1785/gssrl.83.2.250.

Jaeger, J.C., Cook, N.G.W., and Zimmerman, R. 2007. *Fundamentals of Rock Mechanics.* Oxford: Blackwell Publishing Ltd., 4th ed.

Kraft, T., Wiemer, S., Deichmann, N., Diehl, T., Edwards, B., Guilhem, A., Haslinger, F., Király, E., Kissling, E.H., Mignan, A., Plenkers, K., Roten, D., Seif, S., and Woessner, J. 2014. The ML 3.5 earthquake sequence induced by the hydrothermal energy project in St. Gallen, Switzerland. American Geophysical Union, Fall Meeting 2013.

Li, L., and Lee, S.H. 2008. Efficient field-scale simulation of black oil in a naturally fractured reservoir through discrete fracture networks and homogenized media. *SPE REE J.* (August): 750-758.

Majer, E.L., Baria, R., Stark, M., Oates, S., Bommer, J., Smith, B., and Asanuma, H. 2007. Induced seismicity associated with enhanced geothermal systems. *Geothermics,* **36** (3): 185-222. doi: 10.1016/j.geothermics.2007.03.003.

McClure, M.W. and Horne, R.N. 2011. Investigation of injection-induced seismicity using a coupled fluid flow and rate/state friction model. *Geophysics* **76** (6): 181-198. Doi: 10.1190/GEO2011-0064.1.

McClure, M.W. 2012. Modeling and characterization of hydraulic stimulation and induced seismicity in geothermal and shale gas reservoirs. PhD dissertation, Stanford University, Stanford, California, USA (December 2012).

McClure, M.W., and Horne, R.N. 2013. *Discrete Fracture Network Modeling of Hydraulic Stimulation: Coupling Flow and Geomechanics.* Springer. doi: 10.1007/978-3-319-00383-2.

McGarr, A., Bekins, B., Burkhardt, N., Dewey, J., Eartle, P., Ellsworth, W., Ge, S., Hickman, S., Holland, A., Majer, E., Rubinstein, J., and Sheehan, A. 2015. Coping with earthquakes induced by fluid injection. *Science,* **347** (6224): 830 – 831. doi: 10.1126/science.aaa0494.

Mukuhira, Y., Asanuma, H., Niitsuma, H., and Schanz, U. 2008. Characterization of microseismic events with larger magnitude collected at Basel, Switzerland in 2006. Proc., GRC Transactions, **32**.

Norbeck, J., Huang, H., Podgorney, R., and Horne, R. 2014. An integrated discrete fracture model for description of dynamic behavior in fractured reservoirs. Proc., Thirty-Ninth Workshop on Geothermal Reservoir Engineering, Stanford University, Stanford, California, USA, 24-26 Februrary 2014.

Norbeck, J.H., and Horne, R.N. 2014. An embedded fracture modeling framework for fluid flow, geomechanics, and fracture propagation. Proc., International Discrete Fracture Network Engineering Conference, Vancouver, British Columbia, Canada.

Norbeck, J., and Horne, R. 2015. Injection-triggered seismicity: An investigation of porothermoelastic effects using a rate-and-state earthquake model. Proc., Fourtieth Workshop on Geothermal Reservoir Engineering, Stanford, California, USA, 26-28 January.

Segall, P. 2010. *Earthquake and Volcano Deformation.* Princeton University Press, Princeton, New Jersey.

Swiss Seismologic Service. 2013. Earthquake chronology at the geothermal energy project in St. Gallen. URL http://www.seismo.ethz.ch/sed/news/Chronologie_SG/index_EN (accessed 10 November, 2013).

van Poollen, H.K. and Hoover, D.B. 1970. Waste disposal and earthquakes at the Rocky Mountain Arsenal, Derby, Colorado. *Journal of Petroleum Technology* (August): 983-993. SPE-2558-PA. doi: 10.2118/2558-PA.

Zoback, M.D. 2012. "Managing the Seismic Risk Posed by Wastewater Disposal." *Earth* (April): 38-43.